

## Reactivities of Cys<sup>707</sup> (SH1) in Intermediate States of Myosin Subfragment-1 ATPase

Yuichi Hiratsuka, Masumi Eto, Michio Yazawa,<sup>1</sup> and Fumi Morita<sup>2</sup>

Division of Chemistry, Graduate School of Science, Hokkaido University, Sapporo, Hokkaido 060-0810

Received for publication, April 22, 1998

To detect structural changes around the reactive Cys<sup>707</sup> (SH1) in the myosin heavy chain during the ATPase reaction, the reactivity of SH1 in rabbit skeletal myosin subfragment-1 (S-1) was measured using a fluorescent reagent, 5-(iodoacetamidoethyl)aminonaphthalene-1-sulfonic acid, in the presence of various ATP analogs: adenosine 5'-(3-thiotriphosphate) (ATP $\gamma$ S), ADP-vanadate (ADP-V<sub>i</sub>), ADP-BeF<sub>x</sub>, and ADP-AlF<sub>4</sub>. The SH1 reactivities in the S-1 complexes with ATP $\gamma$ S and ADP-BeF<sub>x</sub>, analogs of the E-ATP state, were very high, as well as that in the E-ADP state. In contrast, the SH1 reactivities in the S-1 complexes with ADP-V<sub>i</sub> and ADP-AlF<sub>4</sub>, analogs of the E-ADP-P state, were extremely low. The structural changes around SH1 can be correlated to changes in the structure of the  $\gamma$ -phosphate of ATP during the ATPase reaction or to the structure of the corresponding part of ATP analogs at the active site of ATPase. This is consistent with the crystal structure of S-1 in which the heavy chain structure around SH1 of S-1-ADP-BeF<sub>x</sub> is significantly different from those of S-1-ADP-V<sub>i</sub> and S-1-ADP-AlF<sub>4</sub> [Fisher *et al.* (1995) *Biochemistry* 34, 8960-8972; Smith and Rayment (1996) *Biochemistry* 35, 5404-5417].

**Key words:** ATP analog, ATPase, chemical modification, muscle contraction, myosin subfragment-1.

The energy transduction of myosin is based on intramolecular structural changes of the myosin head coupled to the ATPase reaction. The crystal structure of the truncated *Dictyostelium discoideum* myosin subfragment-1 (S-1) studied by Rayment *et al.* showed that the active site pocket did not change significantly on the binding of various ATP analogs (1-3). They observed, however, that major changes in the three-dimensional structure of the S-1 protein complexed with ADP-AlF<sub>4</sub> and ADP-vanadate (ADP-V<sub>i</sub>) were associated with the C-terminal domain of the S-1 heavy chain. The C-terminal domain forms the interface with the essential light chains, and contains the reactive sulfhydryl groups corresponding to Cys<sup>707</sup> (SH1) and Cys<sup>697</sup> (SH2) (2, 3). This conformational change in the C-terminal domain remote from the active site in the myosin head is thought to be responsible for the power stroke. Consistent changes in the overall shape of the myosin head caused by ATP and analogs have been observed on electron microscopy (4) and X-ray solution scattering (5). Two different shapes (stretched and compact forms) are revealed depending on the type of nucleotides present. Recent three-dimensional reconstitution studies on actin filaments decorated with either smooth

muscle myosin S-1 (6) or brush border myosin I (7) showed major orientational differences in the light chain binding domain of the myosin head upon the addition of ADP. It is likely that the structural changes of the myosin heavy chain around SH1 and SH2 are directly related to such changes in the global shape of the myosin head, since SH1 and SH2 are located nearly in the center of the myosin head (1).

There have been several studies on the structural changes around SH1 of myosin heads induced by ATP or its analogs. Most of these studies involved monitoring of the environments of reporter groups such as fluorophores (8-11) and electron paramagnetic spins (12-14), which were specifically attached to SH1. Chemical cross-linking experiments involving bifunctional reagents also showed that the distance between SH1 and SH2 changed on the addition of ATP, ADP, or actin (15-18).

We attempted to detect differences in the structure around the SH1 region of S-1 associated with various intermediate states during the ATPase cycle. To measure the reactivity of SH1, we selected a method involving a fluorescent reagent, I-AEDANS, which is known to react specifically with SH1 (19, 20). This method is superior to other methods involving chemical probes since only the structure of unmodified S-1 is reflected. ADP-V<sub>i</sub>, ADP-BeF<sub>x</sub>, and ADP-AlF<sub>4</sub> have been shown to form stable complexes which can be regarded as analogs of the steady-state intermediate, E-ADP-P (21-25). Recent crystallographic analyses, however, showed that S-1 complexed with ADP-BeF<sub>x</sub> mimics the ATP bound state, and S-1 complexed with ADP-AlF<sub>4</sub> and ADP-V<sub>i</sub> were assigned as transition state analogs for hydrolysis (2, 3). On the other hand, kinetic studies on the hydrolysis of ATP $\gamma$ S revealed

<sup>1</sup> To whom correspondence should be addressed. E-mail: myazawa@sci.hokudai.ac.jp

<sup>2</sup> Present address: Department of Dairy Science, Rakuno Gakuen University, Ebetsu, Hokkaido 069-0836.

Abbreviations: ATP $\gamma$ S, adenosine 5'-(3-thiotriphosphate); I-AEDANS, 5-(iodoacetamidoethyl)aminonaphthalene-1-sulfonic acid; 2ME, 2-mercaptoethanol; S-1, myosin subfragment-1; V<sub>i</sub>, vanadate ion.

E-ATP $\gamma$ S to be the major steady state intermediate (26). We used, therefore, ATP $\gamma$ S and ADP-BeF $_x$ , ADP-V $_i$  and ADP-AlF $_4$ , as well as ATP and ADP to obtain various intermediate states of S-1 ATPase.

The steady state intermediate, E-ADP-P, and its analogs showed the lowest SH1 reactivity of the S-1 heavy chain. In contrast, analogs of E-ATP, a preceding intermediate, showed the highest SH1 reactivity, which was also shown by E-ADP, the subsequent intermediate. These dramatic changes in SH1 reactivity accompanying the ATPase process coincide with the change in the overall S-1 shape, the rounded form of E-ADP-P and the extended form of the latter two states (5).

#### MATERIALS AND METHODS

**Materials**—5-(Iodoacetamidoethyl)aminonaphthalene-1-sulfonic acid (I-AEDANS), and the sodium salts of ATP and ADP were purchased from Sigma Chemical. ATP $\gamma$ S was purchased from Boehringer Mannheim.

**Proteins**—Myosin was prepared from rabbit skeletal muscle (27). S-1 was prepared from the myosin by digestion with  $\alpha$ -chymotrypsin (28). F-Actin was also prepared from rabbit skeletal muscle (29).

**Determination of the Rate Constant for the Reaction of SH1 with I-AEDANS**—The rate constant was determined by measuring the time-course of the increase in Mg $^{2+}$ -ATPase or Ca $^{2+}$ -ATPase activity of S-1 accompanying the modification of SH1 (30). The modification reactions were started by adding 0.1 to 0.5 mM I-AEDANS to S-1 (0.2 to 1.0 mg/ml) in the presence of 30 mM KCl, 30 mM Tris-HCl (pH 7.5), and 5 mM MgCl $_2$  at 25°C. At several time points during the period from 1 to 4 min, an aliquot of the reaction mixture was transferred to Mg $^{2+}$ - or Ca $^{2+}$ -ATPase assay buffer containing 10 mM dithiothreitol (DTT). ATPase activity in each sample was immediately determined. First-order rate constants for the modification reaction were determined from semilogarithmic plots of the ATPase activity against the reaction time for the modification. Good linear plots were obtained, which indicated a single exponential reaction. The rate constants obtained for the reaction with I-AEDANS were not influenced by the kind of divalent cation used in the ATPase measurements.

**Measurement of ATPase Activity**—ATPase activity was determined by measuring the time-course of P $_i$  liberation. The assay conditions for Mg $^{2+}$ -ATPase (Fig. 1) were 0.2 mg/ml S-1, 1 mM ATP, 0.5 M KCl, 30 mM Tris-HCl (pH 7.5), 5 mM MgCl $_2$ , and 10 mM DTT at 25°C. When S-1 was reacted with I-AEDANS in the presence of actin, the assay conditions for the ATPase were 0.02 mg/ml S-1, 1 mM ATP, 0.5 M KCl, 30 mM Tris-HCl (pH 7.5), 10 mM CaCl $_2$ , 10 mM DTT, 0.1 mg/ml BSA, and 0.3 mM MgCl $_2$  (transferred from the modification medium). The P $_i$  concentration was determined by the method of Ohnishi and Gall (31).

**Confirmation of the Modified Residue (Cys $^{707}$ ) by I-AEDANS**—It has been reported that the presence of ADP increases the reactivity of Cys $^{697}$  (SH2), and that the modification of SH2 results in the complete loss of myosin ATPase activity (32). In our experiments, ATPase activity increased in a single exponential manner after the addition of I-AEDANS and reached a plateau at 10 min with 0.5 mM

I-AEDANS in the presence of 1 mM ADP. The plateau value was maintained for at least 30 min. Therefore, modification of SH2 was unlikely under our conditions. This was also directly confirmed by the SDS-PAGE pattern of the fluorescent peptide bands of AEDANS-S-1 digested by the method of Sutoh (33).

**Preparation of S-1 Complexed with ATP Analogs**—The S-1-ADP-V $_i$  complex and S-1-ADP-metallofluoride complexes were prepared according to the methods of Goodno (21), and Maruta *et al.* (25), respectively. Since the resulting complexes are inactive because of occupation of the active site by these analogs, the amount of a bound ATP analog was determined by measuring the residual Mg $^{2+}$ -ATPase activity of S-1. The S-1-ADP-V $_i$ , S-1-ADP-BeF $_x$ , and S-1-ADP-AlF $_4$  complexes obtained contained 0.90, 0.95, and 0.91 mol of ATP analog/mol of S-1, respectively.

**Preparation of S-1-ADP-V $_i$  Complexes Containing Substoichiometric Amounts of ADP-V $_i$** —S-1-ADP-V $_i$  complexes containing sub-stoichiometric amounts of ADP-V $_i$  were prepared by appropriately interrupting the reaction to form S-1-ADP-V $_i$  as follows. S-1 (20  $\mu$ M) was incubated in 90 mM NaCl, 30 mM Tris-HCl (pH 8.5), 5 mM MgCl $_2$ , 0.2 mM ADP, and 0.25 mM vanadate at 25°C. At several time points during the period from 2 to 22 min, ATP (1 mM in the resulting solution) was added to an aliquot of the reaction mixture to release vanadate or ADP unreacted with the ATPase site of S-1. To remove ATP, free ADP and vanadate ions, each sample (100  $\mu$ l) was immediately applied to a mini-column (300- $\mu$ l bed) of Dowex 1-X8 resin (mesh 100-200) equilibrated with 0.09 M NaCl, 30 mM Tris-HCl (pH 8.5), and 5 mM MgCl $_2$ . After 2 to 3 min, samples were recovered by spinning the resin at 3,000 rpm for 10 s. The ratio of ADP-V $_i$  bound to S-1 was determined by measuring the residual S-1 ATPase activity.

**Comparison of SH1 Reactivities Among S-1s Complexed with Various ATP Analogs**—Reactions with I-AEDANS were started by adding I-AEDANS (0.2 mM in the final reaction mixture) to 0.4 mg/ml S-1-ATP analog complexes, in 250  $\mu$ l of 30 mM KCl, 50 mM Tris-HCl (pH 7.5), and 5 mM MgCl $_2$  at 25°C in the dark. In the case of the complexes with ATP, ADP, and ATP $\gamma$ S, the nucleotides were added before the addition of I-AEDANS. After 2 to 10 min, the reactions were stopped by the addition of 2-mercaptoethanol (2ME) to a final concentration of 2%. Then samples were subjected to SDS-PAGE and the extent of the reaction were determined by measuring the fluorescence intensity of the S-1 heavy chain band using an ATTO AE-6920W densitometer.

**Others**—The concentrations of S-1 and actin were determined from the absorbance at 280 nm using the absorption coefficients, 0.75 and 1.1 (mg/ml) $^{-1}$ ·cm $^{-1}$ , respectively. The concentrations of the S-1-ATP analog complexes were determined by the Bradford method (34) using a standard Bio-Rad protein assay.

#### RESULTS

**Effects of Adenine Nucleotides on the Reactivity of SH1 in S-1**—The reactivity of SH1 in S-1 for I-AEDANS was determined in the absence and presence of ATP or ADP. As shown in Fig. 1, the rate constant for the reaction of SH1 increased linearly with the concentration of I-AEDANS. The reactivity in the presence of ADP was highest, that is,

13 times that in the presence of ATP and 7 times that in the absence of a nucleotide. These results suggest that the structure of S-1 around SH1 changes considerably during the ATPase cycle depending on the conformation of the intermediate species.

**Effects of ATP Analogs on the Reactivity of SH1 in S-1**—We measured the reactivity of SH1 in analogs of intermediate species of ATPase (Fig. 2). Since S-1 complexed with stable ATP analogs does not exhibit ATPase activity, SH1 reactivity was determined from the increase in fluorescence intensity which accompanies the incorporation of the AEDANS group into the S-1 heavy chain ("MATERIALS AND METHODS"). Figure 2, A and B, shows the results of SDS-PAGE indicating the time-courses of the increase in fluorescence intensity. In Fig. 2C and D, the fluorescence intensities are plotted against the reaction time with I-AEDANS. In the presence of ATP, the fluorescence intensity increased gradually with the reaction time, while that in the presence of ADP increased quickly. These SH1 reactivities are consistent with those in Fig. 1 determined from the increase in ATPase activity.

Figure 2 also shows that the reactivity of SH1 in S-1 varies markedly depending on the ATP analog used. Surprisingly, the SH1 reactivity of S-1-ATP $\gamma$ S was as high as that of S-1-ADP (Fig. 2C). The SH1 reactivity of S-1-ADP-BeF $_x$  was also considerably higher than those of S-1-ADP-V $_i$  and S-1-ADP-AlF $_4$  (Fig. 2D), although the increase in fluorescence intensity leveled off at about 60% of the value observed in the presence of ADP. The half-time of the reaction estimated from the increase in fluorescence intensity was almost the same for S-1-ADP and S-1-ADP-BeF $_x$ .

In contrast, very small increases in fluorescence intensity were observed for S-1-ADP-V $_i$  and S-1-ADP-AlF $_4$  (Fig. 2). We then prepared S-1 complexed with sub-stoichiometric amounts of ADP-V $_i$ , and the increase in fluorescence intensity after the addition of I-AEDANS was measured in the presence of 2 mM ADP (Fig. 3). In the presence of ADP, the S-1 species free of ADP-V $_i$  should increase the fluorescence intensity strongly and quickly due to binding of the AEDANS group to SH1 (Fig. 2, C and D), and the reaction

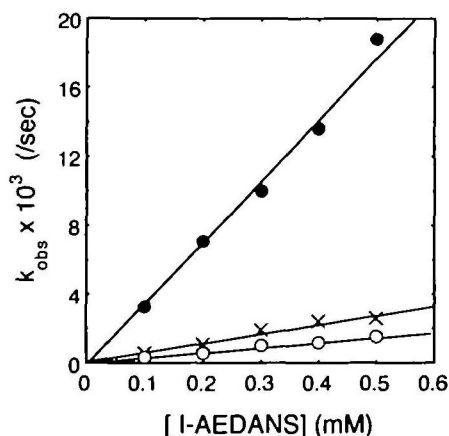


Fig. 1. Reactivity of SH1 in S-1 and effects of ATP and ADP. The rate constants ( $k_{obs}$ ) were determined by measuring the increase in  $Mg^{2+}$ -ATPase activity. The modification with I-AEDANS was performed at 25°C in 30 mM KCl, 30 mM Tris-HCl (pH 7.5), 5 mM MgCl $_2$ , 1.0 mg/ml S-1, and 0.1 to 0.5 mM I-AEDANS (x); in the presence of 1 mM ATP (○); or in the presence of 1 mM ADP (●).

with I-AEDANS should be completed in less than 10 min under these conditions. As shown by the plot in Fig. 3, the fluorescence intensity after 10 min of reaction with I-AEDANS decreased linearly with increases in the amount of ADP-V $_i$  complexes with S-1 in the sample (Fig. 3). These results indicate that the low SH1 reactivity observed with the S-1-ADP-V $_i$  complex (Fig. 2, A and C) is really due to the formation of a complex with ADP-V $_i$  at the active site of S-1. Furthermore, it was found that the reactivity of the real S1-ADP-V $_i$  species estimated by extrapolation to 100% (Fig. 3) was very low, and the reaction was almost non-detectable.

**Reactivity of SH1 in S-1 in the Strong Binding State with F-Actin**—The reactivity of SH1 in S-1 decreased remarkably on the addition of F-actin in both the presence of ADP and the absence of a nucleotide, that is, in the rigor state (Fig. 4). The reactivity in the presence of ADP decreased to one-sixth with an increase in the concentration of F-actin and the decrease levelled off at concentrations of F-actin higher than 5  $\mu$ M. The low SH1 reactivity in the absence of

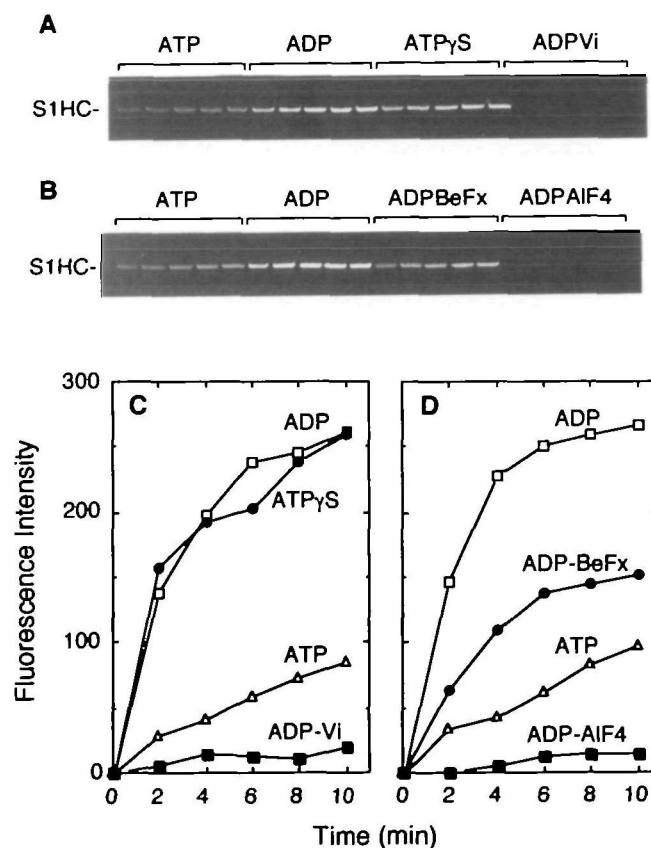


Fig. 2. SH1 reactivities of S-1 complexed with various ATP analogs. The modification reactions were carried out at 25°C in 30 mM KCl, 50 mM Tris-HCl (pH 7.5), 5 mM MgCl $_2$ , 0.4 mg/ml S1-ATP analogs, 0.2 mM I-AEDANS for 2 to 10 min. The S-1-ATP-analog complexes were prepared as described under "MATERIALS AND METHODS." Panels A and B show the results of SDS-PAGE indicating the time courses of the increase in fluorescence intensity of the S-1 heavy chain due to the binding of the AEDANS group to SH1. The reaction was stopped by the addition of 2-ME (2%) every 2 min (from left). The fluorescence intensity was quantified by densitometry and plotted against the reaction time (panels C and D). In panel C: □, ADP; ▲, ATP; ●, ATP $\gamma$ S; ■, ADP-V $_i$ ; and in panel D: ●, ADP-BeF $_x$ ; ■, ADPAIF $_4$ .

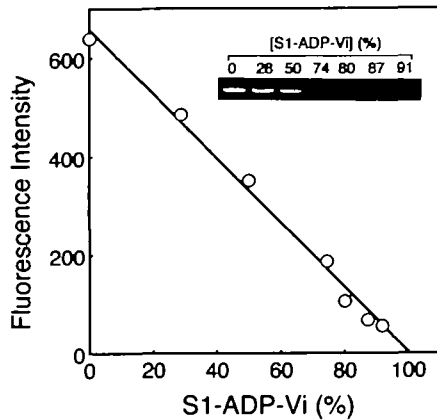


Fig. 3. SH1 reactivities of various S-1-ADP-V<sub>i</sub> preparations. S-1 complexes containing various sub-stoichiometric amounts of ADP-V<sub>i</sub> were prepared as described under "MATERIALS AND METHODS." The fluorescence intensity of the S-1 heavy chain at 10 min after the addition of 0.5 mM I-AEDANS was determined in the presence of 1 mM ADP at 25°C in 30 mM KCl, 50 mM Tris-HCl (pH 7.5), 5 mM MgCl<sub>2</sub>, and 0.4 mg/ml S-1 complex. Under these conditions, it was expected that SH1 of S-1 free of vanadate will be almost completely labeled with the AEDANS group. The inset shows the SDS-PAGE pattern indicating the fluorescence intensity of the S-1 heavy chain after the reaction with I-AEDANS. The numbers indicate the percentages of the S-1 complexed with ADP-V<sub>i</sub>.

both a nucleotide and F-actin (Fig. 1) further decreased to one-fourteenth on the addition of F-actin (Fig. 4).

#### DISCUSSION

**Reactivity of SH1 in S-1 Complexed with ATP Analogs**—As shown in Fig. 1, the largest difference in the reactivity of SH1 in S-1 was observed between the conditions in the presence of ATP and ADP. It has been shown that the steady state intermediate of myosin Mg<sup>2+</sup>-ATPase is E-ADP-P, in which cleavage products ADP and  $\gamma$ -phosphate are both still bound to S-1 (35, 36). Since the most notable difference between S-1 in the presence of ATP and in the presence of ADP is the existence of phosphate corresponding to the  $\gamma$ -position in ATP in the active site, the phosphate at the  $\gamma$ -position has a great effect on the SH1 reactivity. It is, therefore, expected that other states of  $\gamma$ -phosphate observed in different intermediate states may differently affect the local structure of the S-1 heavy chain around SH1.

We compared the SH1 reactivities among S-1 samples complexed with various ATP analogs. Since the cleavage of  $\gamma$ -phosphate is the rate limiting step in the hydrolysis of ATP $\gamma$ S by S-1, the major steady-state intermediate is E-ATP $\gamma$ S in contrast to in the ATPase reaction (26). On the other hand, ADP-V<sub>i</sub>, ADP-BeF<sub>x</sub>, and ADP-AlF<sub>4</sub> have been shown to form analogs of the steady-state intermediate complex, E-ADP-P, in myosin ATPase (21-25). Recent analyses of the crystal structure, however, showed conformational differences between these analogs, and S-1 complexed with ADP-V<sub>i</sub> or ADP-AlF<sub>4</sub> was assigned as an analog in the transition state before the hydrolysis of ATP, while S-1 complexed with ADP-BeF<sub>x</sub> was assigned as an analog of E-ATP (2, 3). Based on these findings, our results in Figs. 1 to 3 indicate that structural changes around SH1 in S-1

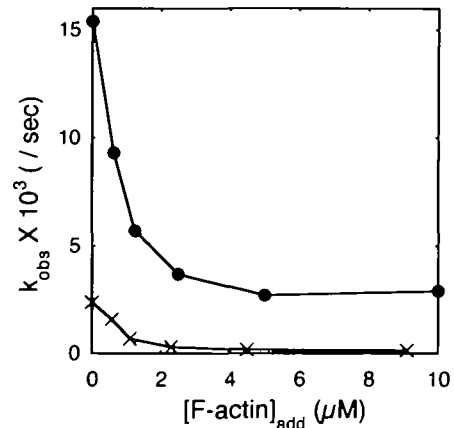


Fig. 4. Effect of F-actin on the reactivity of SH1. The modification was carried out with 0.5 mM I-AEDANS, 30 mM KCl, 30 mM Tris-HCl (pH 7.5), 3 mM MgCl<sub>2</sub>, 0 to 10  $\mu$ M F-actin, and 0.1 mg/ml S-1 at 25°C in the absence ( $\times$ ) or presence ( $\bullet$ ) of 1 mM ADP. The rate constants were obtained by the same method as described in Fig. 1.

may be coupled with the ATPase steps from E-ATP to E-ADP-P, and from E-ADP-P to E-ADP. The high reactivity observed in the presence of ATP $\gamma$ S (Fig. 2C) indicated that the reactivity of SH1 in the S-1-ATP complex was as high as that in the S-1-ADP complex. The reactivity in S-1-ADP-BeF<sub>x</sub> was also as high as that in the S-1-ADP complex, although the maximum increase in fluorescence intensity of the ADP-BeF<sub>x</sub> complex was about one-half that in the case of the ADP-complex (Fig. 2D). This lower fluorescence intensity may be correlated with the reported heterogeneity of the S-1-ADP-BeF<sub>x</sub> complex (23).

In contrast, the SH1 reactivities of S-1-ADP-V<sub>i</sub> and S-1-ADP-AlF<sub>4</sub> were considerably lower (Figs. 2 and 3) than that of S-1 in the presence of ATP, for which the major intermediate species is E-ADP-P (Fig. 2, C and D). This may be due to the presence of 5 to 10% of E-ATP in the steady state of S-1 ATPase (36, 37). The presence, in such small amounts, of E-ATP with the high reactivity of SH1 should increase the apparent SH1 reactivity in the steady state of ATPase, even though the major species, E-ADP-P, exhibits low SH1 reactivity, as do S-1-ADP-V<sub>i</sub> and S-1-ADP-AlF<sub>4</sub>. Therefore, it is likely that the extensive decrease in SH1 reactivity is coupled to the conversion of E-ATP into E-ADP-P or into the transition state for E-ADP-P (2, 3). The structure around SH1 of E-ADP-P is clearly distinguishable from that of the preceding or succeeding intermediate state (E-ATP or E-ADP) in the ATPase cycle. The structures around SH1 of the S-1 heavy chain in E-ATP and E-ADP may be similar with each other judging from the SH1 reactivities.

**Comparison of the SH1 Reactivities of the Various S-1 Complexes to Their Crystal Structures**—Smith and Rayment (3) showed that the three-dimensional structure of the active site pocket of S-1 does not change significantly between the complex with ADP-BeF<sub>x</sub>, and that with either ADP-AlF<sub>4</sub> or ADP-V<sub>i</sub>, while large structural differences were associated with the C-terminal domain of the S-1 heavy chain that contains the reactive SH groups. The C-terminal domain is far from the ATPase active site, that is, several nm in space from the active site. These structural differences in the protein moiety originated from the

structural differences in the  $\gamma$ -phosphate moiety in the active site pocket, that is, whether it is analogous to a trigonal bipyramidal complex resembling the transition state for hydrolysis, or analogous to a tetrahedral complex corresponding to the state before hydrolysis (2, 3). It was interesting to see if these small structural changes in the substrate moiety really had such an effect on the protein structure around SH1, even in solution. The reactivities of SH1 in S-1 complexed with the corresponding analogs showed clear differences (Figs. 2 and 3). These results suggest that the structural changes of the S-1 heavy chain around SH1 occur even in solution depending on the structure of the substrate moiety.

**SH1 Reactivities and the Shape of the Myosin Head**—It has been observed that the overall shape of the myosin head changes to a more compact form on the addition of ATP (4, 5, 38). The results of small-angle X-ray scattering measurement showed that the overall shape of S-1 complexed with ATP $\gamma$ S or ADP was the stretched form, while that with ATP or ADP-V<sub>i</sub> was the compact form (5). These results are consistent with our results as to SH1 reactivity. The S-1 complex having highly reactive SH1 (E-ATP or E-ADP) prefers the stretched form, while the species having unreactive SH1 (E-ADP-P) corresponds to the one with the compact form. These correlations imply that the protein structure around SH1 may be closely related to the overall shape of the myosin head. It has been suggested that the power stroke would be coupled to these structural changes in the myosin head (1, 5, 39). Recently, it was reported that a point mutation at Gly<sup>699</sup>, which is located between SH1 and SH2, caused considerable loss of the motile activity (40), and that the fulcrum point of the swinging motion of the myosin head is located around the SH1-SH2 region based on the results for mutant myosins from *Dictyostelium* with various S-1 neck lengths (41). A network of structural elements similar to that observed around SH1 in the myosin head has also been found in kinesin, another motor protein (42).

**SH1 Reactivity in the Absence of a Nucleotide and the Effect of F-Actin**—As shown in Fig. 4, F-actin considerably decreased the SH1 reactivity in both the presence and absence of ADP. The results may be explained if there are




Species	Reactivity	Shape	State
E <sup>1</sup>	Low		E A-E
		↑↓	
E <sup>2</sup>	High		E-ATP E-ADP
		↑↓	
E <sup>3</sup>	Low		E-ADP-P

Fig. 5. Schematic model of the three S-1 species with SH1 reactivity. This scheme shows the correlation between the reactivity of SH1 in S-1, the shape of the myosin head expected from the results of electron microscopy (4) and X-ray solution scattering (5), and the ATPase intermediate states. E and A denote S-1 and F-actin, respectively.

two different conformations around SH1, and binding of F-actin may shift the equilibrium to stabilize one conformation with much lower reactivity of SH1. Such an equilibrium has been indicated by F-NMR measurements on S-1 with a fluorine-labeled SH1 in the absence of a nucleotide, and one of these states could be dominant in the presence of ADP (43). The low reactivity in the absence of a nucleotide (Fig. 1) may, therefore, reflect the major fraction of the unreactive state, the rest exhibiting high reactivity, which can be dominant in E-ADP.

The SH1 reactivity of the major species of S-1 in the absence of a nucleotide (discussed above) was similar to that of E-ADP-P, and was considerably lower than that observed in the presence of ADP. Therefore, the apparent structure around SH1 of free S-1 is expected to be similar to that observed in the presence of ATP. There is, however, experimental evidence indicating environmental differences around SH1 between S-1s in the presence and absence of ATP (8, 10). Furthermore, chemical cross-linking studies showed that the binding of ATP altered the distance between SH1 and SH2 (15, 16), and that SH1 moved toward the 50-kDa domain on the addition of ATP (17). The overall shape of S-1 is a stretched form in the absence of a nucleotide and is different from the compact round form in the presence of ATP (5). Therefore, the structures around SH1 are probably quite different between S-1s in the presence and absence of ATP, while the difference could not be detected in the present experiments, which revealed similar low reactivity.

**Schematic Model of SH1 Reactivity**—The overall results suggest that there are three different SH1 reactivities in S-1. Figure 5 shows the three different species concerned with these SH1 reactivities, that is, E<sup>1</sup> with low reactivity observed in the absence of a nucleotide or the presence of F-actin, E<sup>2</sup> with the highest reactivity observed in E-ATP and E-ADP, and E<sup>3</sup> with low reactivity observed in E-ADP-P. We suggest that these three species are in equilibrium, which may be affected by the progress of the ATPase reaction or the binding of F-actin. For example, (i) the addition of ATP to S-1 stabilizes E<sup>3</sup> due to the formation of E-ADP-P through E-ATP, that is, E<sup>2</sup>. (ii) The dominant E<sup>3</sup> state of E-ADP-P may shift to the E<sup>2</sup> state of E-ADP with the release of P<sub>i</sub>, which may simultaneously induce a large conformational change of the myosin head (Fig. 5). Then (iii) ADP-release and F-actin binding may shift the equilibrium toward E<sup>1</sup>, as noted in the previous section. The conformational changes responsible for the power stroke may be assigned to a step within the cycle between these three species. The phosphate release step associated with the conversion of E<sup>3</sup> into E<sup>2</sup> may be important for the power stroke, in which the shape of the myosin head changes largely from the compact form to the stretched form. The conformational change around SH1 detected in the present work would be essential for the change in the overall shape of S-1 and the power stroke in muscle contraction.

## REFERENCES

1. Rayment, I., Rypniewski, W.R., Schmidt-Base, K., Smith, R., Tomchick, D.R., Benning, M.M., Winkelmann, D.A., Wesenberg, G., and Holden, H.M. (1993) Three dimensional structure of myosin subfragment-1: A molecular motor. *Science* **261**, 50-58

2. Fisher, A.J., Smith, C.A., Thoden, J.B., Smith, R., Sutoh, K., Holden, H.M., and Rayment, I. (1995) X-ray structures of the myosin motor domain of *Dictyostelium discoideum* complexed with MgADPBeF<sub>3</sub> and MgADPAIF<sub>4</sub>. *Biochemistry* **34**, 8960-8972
3. Smith, C.A. and Rayment, I. (1996) X-ray structure of the magnesium(II). ADP-vanadate complex of the *Dictyostelium discoideum* myosin motor domain to 1.9 Å resolution. *Biochemistry* **35**, 5404-5417
4. Katayama, E. (1989) The effects of various nucleotides on the structure of actin attached myosin subfragment-1 studied by quick-freeze deep-etch electron microscopy. *J. Biochem.* **106**, 751-770
5. Wakabayashi, K., Tokunaga, M., Kohno, I., Sugimoto, Y., Hamanaka, T., Takezawa, T., Wakabayashi, T., and Amemiya, Y. (1992) Small-angle synchrotron X-ray scattering reveals distinct shape changes of the myosin head during hydrolysis of ATP. *Science* **258**, 443-447
6. Whittaker, M., Wilson-Kubalek, E.M., Smith, J.E., Faust, L., Milligan, R.A., and Sweeney, H.L. (1995) A 35-Å movement of smooth muscle myosin on ADP release. *Nature* **378**, 748-751
7. Jontes, J.D., Wilson-Kubalek, E.M., and Milligan, R.A. (1995) A 32 degree tail swing in brush border myosin I on ADP release. *Nature* **378**, 751-753
8. Aguirre, F.G., Gonsoulin, F., and Cheung, H.C. (1986) Interaction of fluorescently labeled myosin subfragment 1 with nucleotides and actin. *Biochemistry* **25**, 6827-6835
9. Ajtai, K. and Burghardt, T.P. (1987) Probe studies of the MgADP state of muscle cross-bridges: Microscopic and wavelength-dependent fluorescence polarization from 1,5-IAEDANS-labeled myosin subfragment-1 decorating muscle fibers. *Biochemistry* **26**, 4517-4523
10. Hiratsuka, T. (1993) Behavior of Cys-707 (SH1) in myosin associated with ATP hydrolysis revealed with a fluorescent probe linked directly to the sulfur atom. *J. Biol. Chem.* **268**, 24742-24750
11. Berger, C.L., Craik, J.S., and Trentham, D.R. (1995) Fluorescence polarization from isomers of tetramethylrhodamine at SH-1 in rabbit psoas muscle fibers. *Biophys. J.* **68**, 78S-80S
12. Fajer, P.G., Fajer, E.A., Matta, J.J., and Thomas, D.D. (1990) Effect of ADP on the orientation of spin-labeled myosin heads in muscle fibers: A high-resolution study with deuterated spin labels. *Biochemistry* **29**, 5865-5871
13. Raucher, D., Sar, C.P., Hideg, K., and Fajer, P.G. (1994) Myosin catalytic domain flexibility in MgADP. *Biochemistry* **33**, 14317-14323
14. Ponomarev, M.A., Timofeev, V.P., and Levitsky, D.L. (1995) The difference between ADP-beryllium fluoride and ADP-aluminum fluoride complexes of the spin-labeled myosin subfragment 1. *FEBS Lett.* **371**, 261-263
15. Burke, M. and Reisler, E. (1977) Effect of nucleotide binding on the proximity of the essential sulfhydryl groups of myosin. Chemical probing of movement of residues during conformational transitions. *Biochemistry* **16**, 5559-5563
16. Wells, J.A., Knoeber, C., Sheldon, M.C., Werber, M.M., and Yount, R.G. (1980) Cross linking of myosin subfragment 1. Nucleotide-enhanced modification by a variety of bifunctional reagent. *J. Biol. Chem.* **255**, 11135-11140
17. Lu, R.C., Moo, L., and Wong, A.G. (1986) Both the 25-kDa and 50-kDa domains in myosin subfragment 1 are close to the reactive thiols. *Proc. Natl. Acad. Sci. USA* **83**, 6392-6396
18. Blotnick, E. and Muhrad, A. (1994) Effect of nucleotides and actin on the intramolecular cross-linking of myosin subfragment-1. *Biochemistry* **33**, 6867-6876
19. Duke, J., Takashi, R., Ue, K., and Morales, M.F. (1976) Reciprocal reactivities of specific thiols when actin binds to myosin. *Proc. Natl. Acad. Sci. USA* **73**, 302-306
20. Takashi, R., Duke, J., Ue, K., and Morales, M.F. (1976) Defining the "fast-reacting" thiols of myosin by reaction with 1,5-IAEDANS. *Arch. Biochem. Biophys.* **175**, 279-283
21. Goodno, C.C. (1979) Inhibition of myosin ATPase by vanadate ion. *Proc. Natl. Acad. Sci. USA* **76**, 2620-2624
22. Phan, B. and Reisler, E. (1992) Inhibition of myosin ATPase by beryllium fluoride. *Biochemistry* **31**, 4787-4793
23. Werber, M.M., Peyser, Y.M., and Muhrad, A. (1992) Characterization of stable beryllium fluoride, aluminum fluoride, and vanadate containing myosin subfragment 1-nucleotide complexes. *Biochemistry* **31**, 7190-7197
24. Phan, B.C., Faller, L.D., and Reisler, E. (1993) Kinetic and equilibrium analysis of the interactions of actomyosin subfragment-1 ADP with beryllium fluoride. *Biochemistry* **32**, 7712-7719
25. Maruta, S., Henry, G.D., Sykes, B.D., and Ikebe, M. (1993) Formation of the stable myosin-ADP-aluminum fluoride and myosin-ADP-beryllium fluoride complexes and their analysis using <sup>19</sup>F-NMR. *J. Biol. Chem.* **268**, 7093-7100
26. Bagshaw, C.R., Eccleston, J.F., Trentham, D.R., Yates, D.W., and Goody, R.S. (1972) Transient kinetic studies of the Mg<sup>2+</sup>-dependent ATPase of myosin and its proteolytic subfragments. *Cold Spring Harbor Symp. Quant. Biol.* **37**, 127-135
27. Perry, S.V. (1955) Myosin adenosinetriphosphatase in *Methods in Enzymology* (Colowick, S.P. and Kaplan, N.O., eds.) Vol. 2, pp. 582-588, Academic Press, New York
28. Onodera, M. and Yagi, K. (1971) Studies on enzymatically active subfragments of myosin-adenosine triphosphatase. I. Preparation using chymotrypsin. *J. Biochem.* **69**, 145-153
29. Spudich, J.A. and Watt, S. (1971) The regulation of rabbit skeletal muscle contraction. I. Biochemical studies of the interaction of the tropomyosin-troponin complex with actin and the proteolytic fragments of myosin. *J. Mol. Biol.* **246**, 4866-4871
30. Sekine, T. and Kielly, W.W. (1964) The enzymatic properties of N-ethylmaleimide modified myosin. *Biochim. Biophys. Acta* **81**, 336-345
31. Ohnishi, S.T. and Gall, R.S. (1978) Characterization of the catalyzed phosphate assay. *Anal. Biochem.* **88**, 347-356
32. Yamaguchi, M. and Sekine, T. (1966) Sulfhydryl groups involved in the active site of myosin A adenosine triphosphatase. I. Specific blocking of the SH group responsible for the inhibitory phase in "B phasic response" of the catalytic activity. *J. Biochem.* **59**, 24-33
33. Sutoh, K. (1981) Location of SH1 and SH2 along a heavy chain of myosin subfragment 1. *Biochemistry* **20**, 3281-3285
34. Bradford, M.M. (1976) A rapid and sensitive method for the quantitation of microgram quantities of protein utilizing the principle of protein-dye binding. *Anal. Biochem.* **72**, 248-254
35. Taylor, E.W., Lyman, R.W., and Moll, G. (1970) Myosin-product complex and its effect on the steady-state rate of nucleotide triphosphate hydrolysis. *Biochemistry* **9**, 2984-2991
36. Bagshaw, C.R. and Trentham, D.R. (1974) The characterization of myosin-product complexes and product-release steps during the magnesium ion-dependent adenosine triphosphatase reaction. *Biochem. J.* **141**, 331-349
37. Taylor, E.W. (1977) Transient phase of adenosine triphosphate hydrolysis by myosin, heavy meromyosin, and subfragment-1. *Biochemistry* **16**, 732-740
38. Craig, R., Green, L.E., and Eisenberg, E. (1985) Structure of the actin-myosin complex in the presence of ATP. *Proc. Natl. Acad. Sci. USA* **82**, 3247-3251
39. Spudich, J.A. (1994) How molecular motors work. *Nature* **372**, 515-518
40. Kinose, F., Wang, S.X., Kidambi, U.S., Moncman, C.L., and Winkelmann, D.A. (1996) Glycine 699 is pivotal for the motor activity of skeletal muscle myosin. *J. Cell Biol.* **134**, 895-909
41. Uyeda, Q.P.T., Abramson, P.D., and Spudich, J.A. (1996) The neck region of the myosin motor domain acts as a lever arm to generate movement. *Proc. Natl. Acad. Sci. USA* **93**, 4459-4464
42. Kull, F.J., Sablin, E.P., Lau, R., Fletterick, R.J., and Vale, R.D. (1996) Crystal structure of the kinesin motor domain reveals a structural similarity to myosin. *Nature* **380**, 550-555
43. Shriver, J.W. and Sykes, B.D. (1982) Energetics of the equilibrium between two nucleotide-free myosin subfragment 1 states using fluorine-19 nuclear magnetic resonance. *Biochemistry* **21**, 3022-3028